

Low-cycle fatigue in Ni₃Al-based alloys

D. E. GORDON, C. K. UNNI

General Dynamics, Fort Worth Division, PO Box 748, Fort Worth, TX 76101, USA

The low-cycle fatigue properties of hot-extruded powders of a Ni₃Al-based alloy, IC 218, with nominal composition Ni-16.5Al-8.0Cr-0.4Zr-0.1B (at %) have been evaluated at room temperature. Tests were conducted under total strain conditions in a laboratory air environment. Results indicate that the low-cycle fatigue performance of the PM processed IC 218 nickel aluminide is superior to other structural alloys especially at higher strain amplitudes. These results are explained in terms of the high ductility of the fine-grain material and good crack growth propagation resistance in these alloys. Stress response curves for annealed IC 218 alloys indicate considerable cyclic hardening followed by cyclic softening. The onset of cyclic softening is found to occur at a constant cumulative plastic strain. The critical cumulative plastic strain criteria are verified for step-loaded IC 218 nickel aluminide coupons.

1. Introduction

The recent interest in ductile intermetallic compounds has resulted in considerable development of alloys based on Ni₃Al. Polycrystalline alloys with a sub-stoichiometric aluminium content exhibit good room-temperature ductility when alloyed with 0.1-0.25 at % B [1-3]. It has been shown that solid solution strengthening with hafnium and zirconium can be effective in improving the mechanical properties of these alloys [4, 5]. Alloying with iron and chromium has been extensively studied, and improved strength and oxidation and sulphidation resistance are reported for alloys containing these elements [5-7]. Elevated temperature testing in air has shown that Ni₃Al is sensitive to dynamic oxygen embrittlement in the temperature range 600-800 °C; however, this effect can be minimized by reducing the aluminium content or alloying with about 8 wt % Cr [6, 8].

The tensile properties of hot-extruded powders of Ni-17.4Al-7.9Cr-0.5Zr-0.07B (at %), an alloy similar to IC 218, was evaluated from room temperature to 1000 °C [9]. The fine-grained material from extruded aluminide powder had room-temperature strengths above those which are usually obtainable with cast materials while retaining good ductility. The increment of increase in yield stress on increasing temperature was relatively small in the powder material. The two-phase alloy containing chromium and zirconium showed very little evidence of dynamic oxygen embrittlement with elongations greater than 30% being reported from 25-800 °C [9]. The effects of preoxidation are quite different for large-grained Ni₃Al-based alloys compared to fine-grained material. Embrittlement has been reported in large-grained alloys at 760 °C after preoxidation [10, 11]. In the fine-grained material, however, no effect on ductility at 760 °C was observed after elevated temperature exposures in air [10, 11].

Recent fatigue investigations in Ni₃Al-based alloys have involved mainly crack growth resistance [12, 13] and high-cycle fatigue studies [14, 15]. In terms of crack growth resistance, (da/dn), Ni₃Al-based alloys displayed excellent resistance to fatigue crack propagation and compared favourably with other structural alloys tested under similar conditions at 600 °C [12, 13]. In high-cycle fatigue, Ni₃Al-based alloys exhibited high ratios of fatigue limit to tensile yield stress at 25 and 500 °C [14, 15]. This behaviour was explained in terms of rapid cyclic hardening and delayed crack initiation in these alloys [15]. Most of the work in low-cycle fatigue has been restricted to Ni₃Al single crystals where asymmetric effects have been observed [16].

This paper presents the results of a study of the low-cycle fatigue properties of hot-extruded powders of a Ni₃Al-based alloy, IC 218. This alloy was developed by Oak Ridge National Laboratory with nominal composition of Ni-16.5Al-8.0Cr-0.4Zr-0.1B (at %). Cyclic hardening and softening behaviour as determined from strain-controlled experiments was related to fatigue life in this alloy. Powder-metallurgy (PM) produced components often quite easily achieve equivalent static mechanical properties of wrought material. However, the desired low-cycle fatigue (LCF) properties of PM produced parts are often difficult to achieve. The LCF test, particularly at high strain levels, is sensitive to any microstructural discontinuity including foreign particle inclusions, voids, and characteristics resulting from thermal treatments [17].

2. Experimental procedure

Powders produced by vacuum gas atomization were obtained from Homogeneous Metals Incorporated, Clayville, NY. The powders were sealed in evacuated steel cans and extruded at 1100 °C. Reduction ratio

TABLE I Chemical composition (wt %)

Alloy	Ni	Al	Cr	Zr	B	O ₂	N ₂	C	S
IC 218	83.2	8.2	7.8	0.80	0.017	0.013	0.001	< 0.005	< 0.002

TABLE II Low-cycle fatigue results

Total strain range $\Delta\epsilon_T$ (%)	Plastic strain range, $\Delta\epsilon_p$, at $N_f/2$ (%)	Elastic strain range, $\Delta\epsilon_e$, at $N_f/2$ (%)	N_i (cycles)	N_f (cycles)	Maximum stress at $N_f/2$ (MPa)	E (GPa)
4.00	2.98	1.02	828	855	1107	216
3.60	2.58	1.02	883	905	1106	221
2.80	1.83	0.97	1140	1157	1067	218
2.80	1.81	0.99	1340	1373	1075	216
2.40	1.43	0.97	2451	2471	1081	225
2.00	1.02	0.98	3188	3190	1057	218
1.40	0.55	0.85	4573	4738	939	225
1.30	0.44	0.86	12658	12788	896	218
1.10	0.29	0.81	20466	20526	877	223

was 14:1. Extrusion was done with - 325 mesh powder. The chemical composition of the IC 218 material is given in Table I. Test coupons were obtained from extruded rods. The samples were annealed for 1 h at 1000 °C in a vacuum prior to testing to produce an equiaxed microstructure.

ASTM E606 axial fatigue specimens were used for conducting fully reversed, $R = -1$, constant amplitude LCF tests under total axial strain control. A triangular wave form and a test frequency of 10 c.p.m. was used. The test section of each specimen was polished manually in the axial direction to remove circumferential scratches.

3. Results

The microstructure of the extruded IC 218 alloy is shown in Fig. 1. A very fine grain size was observed after extrusion. After annealing for 1 h at 1000 °C, an equiaxed microstructure with an average grain size of approximately 8 μm was obtained. The microstructure of the Ni₃Al + Cr + Zr alloys has been found to consist of disordered islands of γ within an ordered γ' matrix after the final heat treatment [5].

Tensile properties were measured in the powder-extruded alloy for temperatures ranging from 25–850 °C (Fig. 2). Relatively high ductility was observed throughout the temperature range with elongations of $\approx 30\%$ measured between 25 and 650 °C. The increment of change in yield stress on increasing temperature was relatively small up to 850 °C. A continuous decrease in ultimate tensile strength was observed with increase in temperature.

Low-cycle fatigue results are shown in Table II. Total strain ranges, $\Delta\epsilon_T$, plastic strain ranges at $N_f/2$, $\Delta\epsilon_p$, and elastic strain ranges at $N_f/2$, $\Delta\epsilon_e$, are presented. Both N_i and N_f are listed where N_i is defined as the number of cycles where a significant change in tensile load or plastic strain signal was detected and

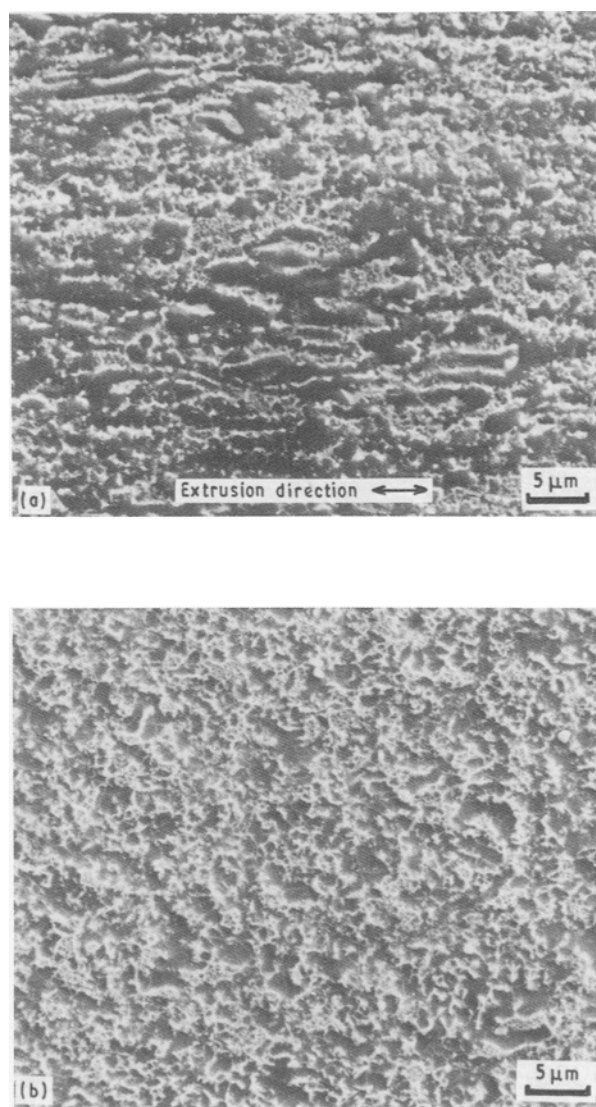


Figure 1 Microstructure of extruded IC 218 alloys. (a) Cross-section showing microstructure parallel to extrusion direction. (b) Cross-section showing microstructure perpendicular to extrusion direction.

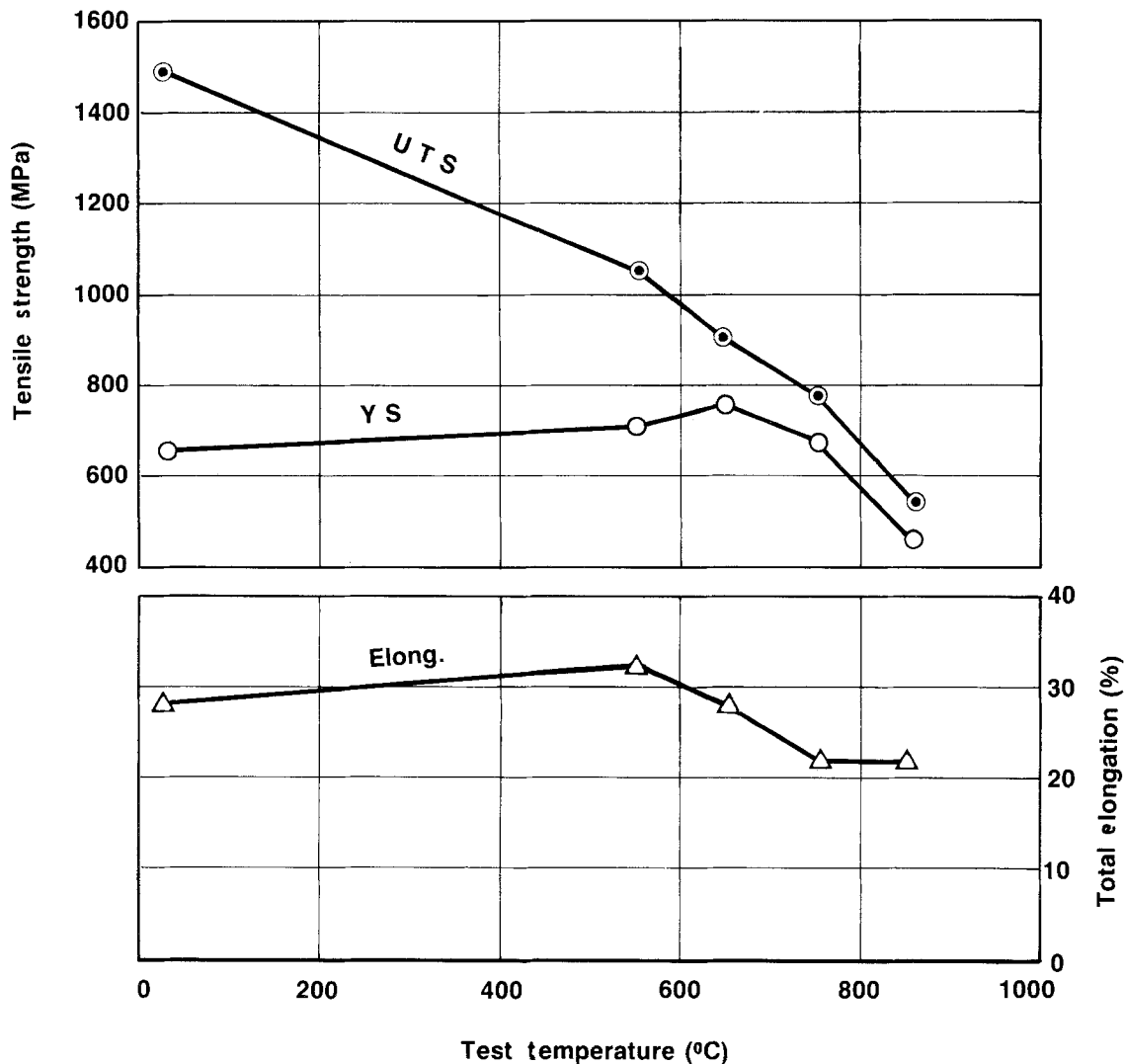


Figure 2 Monotonic tensile properties as a function of test temperature.

N_f is the number of cycles to failure. The maximum stress at $N_f/2$ and modulus are also shown in Table II.

Upon initial cycling, all of the test coupons exhibited large yield drops, before uniform elongation began. This phenomenon has been observed in tensile tests for this type of alloy [9] where Lüders strains as large as 5% were observed. After the initial drop in yield strength, considerable cyclic hardening occurred followed by cyclic softening particularly at larger total strain amplitudes. Plastic strain amplitudes varied considerably in early cycling due to this rapid cyclic hardening. The rapid cyclic hardening was followed by cyclic softening which was somewhat less pronounced. Values of $\Delta\epsilon_p$ are shown in Table II at $N_f/2$. In general, only small changes in plastic strain amplitude were observed from $N_f/2$ until fatigue failure occurred.

Strain-life data are plotted in Fig. 3 showing the total strain amplitude and the elastic and plastic strain components as a function of reversals to failure ($2N_f$). The Coffin-Manson strain-life approximation given by

$$\frac{\Delta\epsilon_T}{2} = \frac{\sigma'_f}{E}(2N_f)^b + \epsilon'_f(2N_f)^c \quad (1)$$

was found to predict accurately the LCF behaviour of IC 218 nickel aluminide, as linear slope behaviour was

observed. Calculated values of the cyclic parameters, ϵ'_f , c , σ'_f and b , are also shown. The parameters ϵ'_f and σ'_f were determined by extrapolation of the plastic and elastic strain curves, respectively, to $2N_f = 1$ reversal. The parameters c and b are the slopes of the plastic and elastic strain curves, respectively.

Often in the absence of adequate data on constant-strain-amplitude fatigue, low-cycle fatigue parameters have been estimated from monotonic tensile properties. These approximations have been found to be fairly accurate for steels of various hardnesses [18, 19]. If these approximations are applied to LCF results for the IC 218 nickel aluminide, the following results are obtained. The fatigue ductility coefficient is often set equal to the true fracture ductility, $\epsilon'_f \approx \epsilon_f$. In the IC 218 alloy, the fatigue ductility coefficient, $\epsilon'_f \approx \ln(1/1-RA)$ would indicate a quite large reduction of area ($RA \approx 92\%$) for the powder-extruded IC 218 alloy. Tensile elongations of 28% have been measured in this alloy; therefore, based on the high ductility of the fine-grained material, a large value of fatigue-ductility coefficient would be expected. The fatigue-strength coefficient can be approximated by $\sigma'_f \approx \sigma_f$ (corrected for necking), or for many materials, σ'_f (MPa) $\approx (\sigma_{ult.} + 348)$ [18]. In the IC 218 alloy, $\sigma'_f = 1865$ MPa, which would denote an ultimate tensile

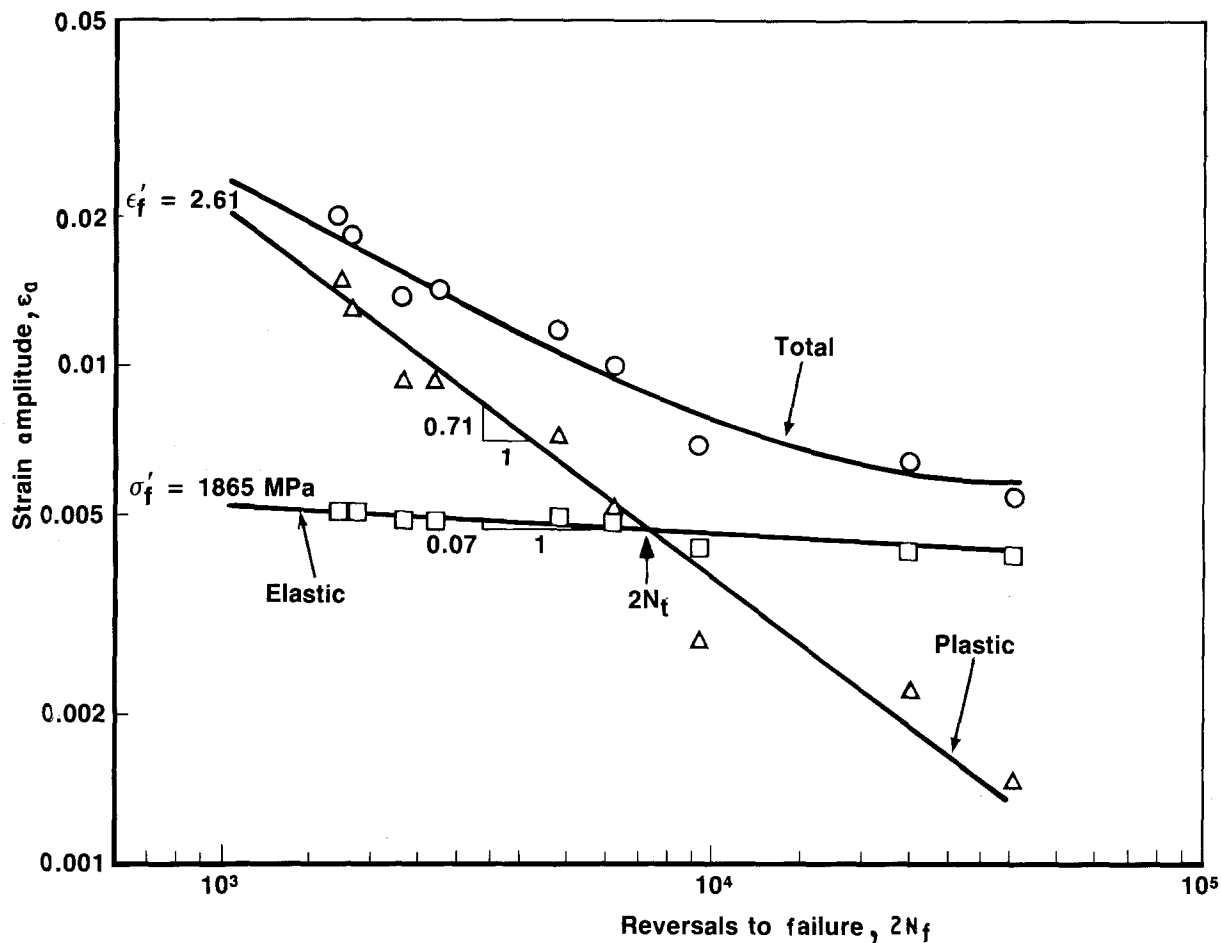


Figure 3 Elastic, plastic, and total strain amplitude-fatigue life behaviour of IC 218 nickel aluminide.

strength of 1517 MPa. An ultimate tensile strength of 1497 MPa has been measured which is in excellent agreement. The fatigue strength exponent $b = -0.07$, obtained from the slope of the elastic strain curve, is fairly low compared to most materials where b varies from -0.05 to -0.12 . The value of b can be approximated from the relation, $b \approx -1/6 \log(2\sigma_f/\sigma_{ult.})$ [18]. Using this approximation, the value $b = -0.065$ is obtained which is in fairly close agreement to the experimental value found. Materials which can work extensively such as annealed IC 218 nickel aluminide normally have low absolute magnitudes of b , with little effect on σ_f' . These low absolute values for b are normally associated with increasing long-life fatigue strength. The fatigue-ductility coefficient, c , is not as well-defined as are the other fatigue parameters. Morrow has shown that for many metals, c varies between -0.5 and -0.7 [20]. The value, $c = -0.71$, obtained for this alloy is slightly higher than obtained for most metals. Estimating c from monotonic tensile properties, $c \approx b - \log(\epsilon_f' E/\sigma_f')/\log(2N_t)$. In certain steels, the transition fatigue life, $2N_t$, can be estimated from the hardness [18]. The measured hardness of the annealed IC 218 alloy was 281 HB. This hardness corresponds to a transition fatigue life of ≈ 7500 reversals [18]. Using this value for $2N_t$, a calculated value of $c = -0.705$ was obtained. This value is in close agreement to the experimental value, $c = -0.71$.

In terms of gas-turbine disc LCF life, the transition fatigue life, N_t , i.e. LCF life where elastic and plastic

strains are equal, is an important factor [21]. For LCF life greater than N_t , elastic strain predominates whereas for LCF life, lower than N_t , plastic strain predominates. The N_t value for this alloy was of the order of 3700 cycles. The value of $2N_t$ (7400 reversals) can be reasonably approximated from the transition fatigue life versus hardness curve used for ferrous alloys [18].

A comparison of total strain amplitude versus cycles-to-failure for IC 218 with other alloys (Fig. 4) indicates that the low-cycle fatigue performance of IC 218 nickel aluminide at 25 °C compares favourably with other structural alloys especially at higher strain amplitudes. Ductility and fatigue crack propagation resistance are dominating factors at high strain amplitudes; therefore, this behaviour is not unexpected. At lower strain amplitudes where strength plays a dominant part, fatigue performance of the annealed IC 218 alloy was better than expected based on its relatively low monotonic yield strength (654 MPa). Also shown in Fig. 3 are low-cycle fatigue curves for several steels [22], and PREP Ti-6Al-4V [23]. No LCF data are available for wrought Ni₃Al-based alloys at 25 °C; therefore, no comparison could be made between PM processed and wrought material.

Stress response curves for annealed IC 218 alloy indicate considerable cyclic hardening followed by cyclic softening (Fig. 5). For example, maximum tensile stresses increased nearly 100% during the first 15 cycles at a total strain amplitude of $\Delta\epsilon_T/2 = 1.6\%$. At the lower strain amplitude, $\Delta\epsilon_T/2 = 0.7\%$, hardening occurred for a larger number of cycles (≈ 90) before

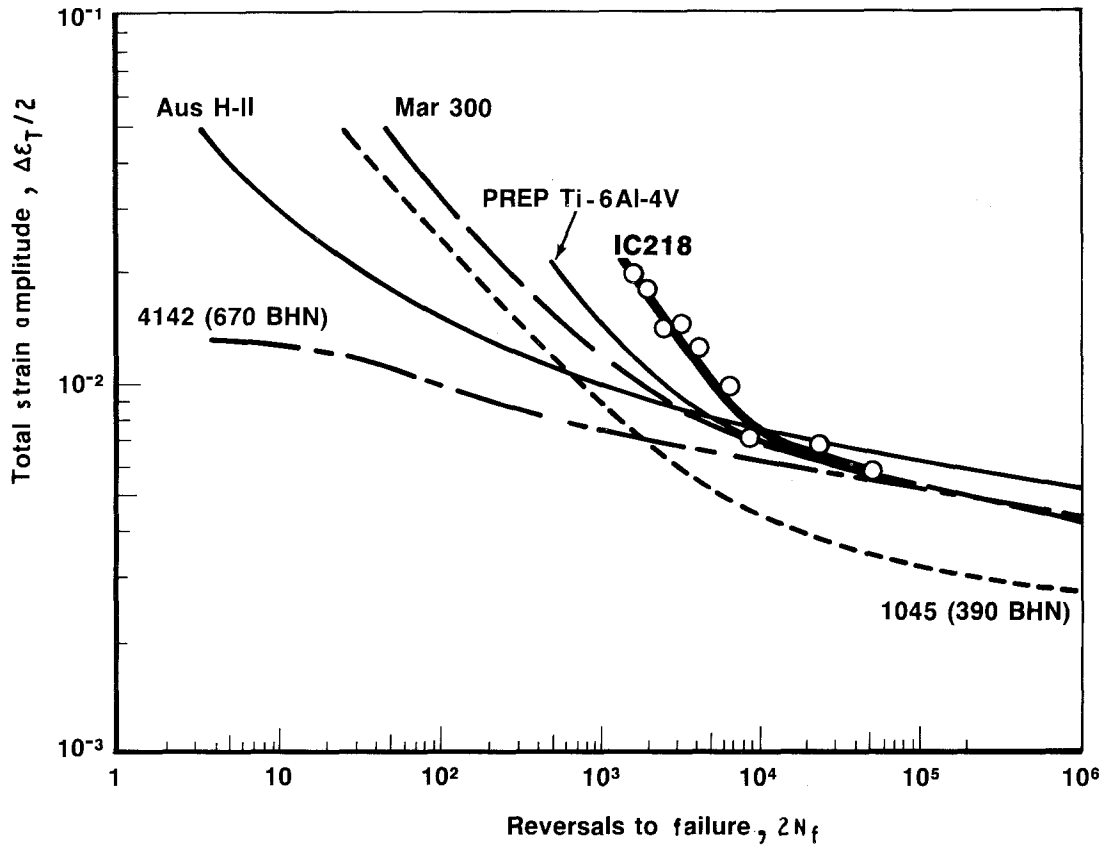


Figure 4 Representative strain-life behaviour for different alloys. Steel data from [22], PREP Ti-6Al-4V data from [23].

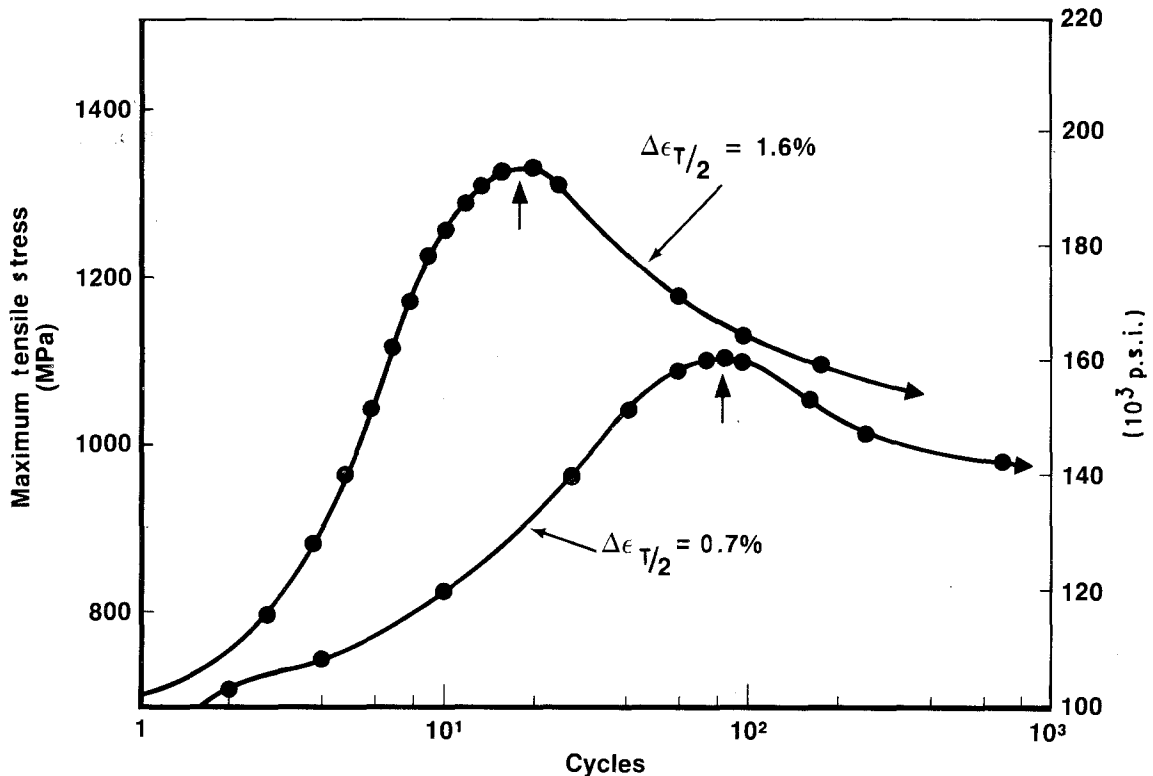


Figure 5 Stress response curves for annealed IC 218 alloys.

softening initiated. The number of cycles to maximum hardening, $N(\sigma_{max})$, increased with decrease in strain and was found to occur at a critical cumulative plastic strain, $N(\sigma_{max})\epsilon_p \approx 34\%$, regardless of strain amplitude (Table III). The onset of cyclic softening is suggested to occur at this constant cumulative plastic strain.

The critical cumulative plastic strain criteria were verified for annealed IC 218 alloy samples step-loaded. Again, the accumulated plastic strains before cyclic hardening stops were approximately the same as obtained in samples that were not step-loaded (Table III).

TABLE III Cumulative plastic strain before cyclic softening starts

Sample (no.)	Cycles before maximum stress	$N(\sigma_{\max})\epsilon_p$ (%)	Ave
1	16	32.0	
2	19	28.0	
3	25	39.0	33.5
4	74	35.0	
5 (Step-loaded)	–	36.0	
6 (Step-loaded)	–	32.0	34.0

4. Discussion

The fine-grained material which results from extrusion of powders has good low-cycle fatigue properties at 25 °C. The superior LCF life (in terms of plastic strain range) can be attributed to the finer grain size, which promotes homogeneous deformation and retards crack nucleation by reducing stress concentrations. Because no LCF data are available for wrought nickel aluminide alloys at room temperature, direct comparisons between PM processed and wrought material could not be made.

Models have been developed using LCF parameters for predicting crack growth rates [24–26]. These models assume that for a ductile material and proper ΔK range, fatigue crack growth occurs by exhaustion of ductility due to cyclic plastic strain in the reverse plastic zone ahead of the crack tip. Comparisons of predicted crack growth curves using these models with FCP data obtained experimentally show good agreement for intermediate and high values of ΔK for several alloy systems [25]. However, at low ΔK values or near threshold, the plastic strain at a given distance from the crack tip also depends on a microstructural parameter, ρ , which is related to slip distance. Using low-cycle fatigue parameters derived for IC 218 (Fig. 3 and Table II), crack growth rates were calculated from a model for measuring fatigue crack growth developed by Majumdar and Morrow [26]. These values were compared to experimental crack growth rates measured for a similar alloy, IC 221, at room temperature [12]. For intermediate and high ΔK values, agreement between calculated da/dn values and experimental values for IC 221 was reasonably good. For lower ΔK values, near threshold, the model overestimates the crack growth rate.

Cyclic hardening followed by cyclic softening has been observed in ordered alloys such as Ni_3Mn [27]. This effect has been interpreted as the breakdown of the long-range ordered structure. However, in this case, the life is not decreased, because ordering results in a more planar slip character and a resultant homogenization of slip which outweighs any effects of strain concentration due to local softening. A number of other alloys exhibit similar cyclic response behaviour, although the magnitude of the cyclic hardening is normally smaller. Nickel-base alloys strengthened by γ'' [28] and Al–Cu alloys strengthened by θ'' [29] exhibit similar behaviour. Softening is thought to occur in these alloys through a disruption of local,

ordered atomic arrangement. This atomic rearrangement results in a reduction locally in the amount of ordered phase and a loss in the order contribution to strengthening [30].

Cyclic hardening/softening behaviour under $R = -1$ loading has been found to correlate with high-cycle fatigue behaviour [31]. For alloys exhibiting a large amount of cyclic hardening, quite large ratios of $\Delta\sigma$ (at 10^6 cycles)/ σ_{YS} are observed. On the contrary, cyclic softening normally leads to poorer high-cycle fatigue (HCF) performance. Plastic strains generated under stress-controlled high-cycle fatigue should be relatively small under long-life conditions. Cyclic hardening behaviour would be expected to predominate in the IC 218 alloy throughout most or all of the fatigue lifetime allowing strains to be reduced for a constant stress amplitude thus prolonging fatigue life.

The effects of ordering on strain-controlled fatigue under tension/compression loading ($R = -1$) is less well defined. The elastic strain parameters, particularly b , are improved due to cyclic hardening. Long-life strain resistance is determined by the same parameters indicative of stress behaviour (elastic behaviour). Plastic strain parameters (ϵ_f' and c), are hurt as a result of cyclic hardening where some plasticity is present. The Coffin–Manson behaviour of the cyclic hardening alloy will be inferior to the fatigue life of cyclic stable or cyclic softening alloy. Under these conditions, a reversal of behaviour in stress control versus strain control can be observed. At higher strain amplitudes under strain-controlled conditions, the plastic strain behaviour in the IC 218 is apparently improved due to the cyclic softening that follows initial hardening.

The critical cumulative plastic strain criteria observed in the IC 218 nickel aluminide has been observed in several alloy systems. Calabrese and Laird [29] observed similar results in an Al–4% Cu alloy aged to contain θ'' precipitates. In the Al–4% Cu alloy, hardening first occurred by dislocation accumulation throughout the material and softening occurred when the slip was subsequently localized, yielding persistent slip bands (PZBs). The cyclic response of Waspalloy has been found to be a function of γ' precipitate size [32]. Specimens with precipitates larger than the critical size for dislocation bowing (50 and 90 nm) cyclically harden to a saturation stress value much like the IC 218 material system. Material with smaller, shearable precipitates (8 nm) hardened to a maximum stress, then markedly softened. Unlike in the IC 218 alloy, the number of cycles to maximum stress was constant with plastic strain in the 8 nm material. Similar behaviour to Waspalloy with small, shearable precipitates has been observed in the Udimet 700 alloy where the number of cycles to maximum hardening was a constant, independent of the plastic strain [28].

5. Conclusions

The fine-grained material from extruded IC 218 nickel aluminide powders has excellent room-temperature

low-cycle fatigue properties especially at high strain amplitudes. These results can be explained in terms of the high ductility of the fine-grained microstructure. These results would also be expected based on fatigue crack propagation results at room-temperature for a similar alloy, IC 221 [12].

Low-cycle fatigue properties in the IC 218 alloy can be reasonably approximated from monotonic tensile properties. Techniques developed for estimating the cyclic properties for steels when only the tensile properties are known also give reasonable values for the cyclic parameters in the IC 218 nickel aluminide.

Stress response curves for annealed IC 218 alloys indicated considerable cyclic hardening followed by cyclic softening. The onset of cyclic softening was found to occur at a constant cumulative plastic strain. The critical cumulative plastic strain criteria were verified for step-loaded IC 218 nickel aluminide coupons.

Acknowledgements

This work was supported by General Dynamics Independent Research and Development. The authors thank Dr N. S. Stoloff, Rensselaer Polytechnic Institute, for helpful discussions and supplying crack growth propagation resistance data on IC 221 nickel aluminide before publication; Dr W. R. Garver for support of this research and reviewing the manuscript, and also Drs V. K. Sikka and C. T. Liu, Oak Ridge National Laboratory, for helpful discussions.

References

1. K. AOKI and P. IZUMI, *Nippon Kinzoku, Takkaiishi* **43** (1979) 1190.
2. C. T. LIU and J. O. STIEGLER, *Science* **226** (1984) 636.
3. C. T. LIU, C. L. WHITE and J. A. HORTON, *Acta Metall.* **33** (1985) 213.
4. C. T. LIU and C. L. WHITE, in "Materials Research Society Symposium Proceedings on High Temperature Ordered Intermetallic Alloys", Vol. 39, edited by C. C. Koch (Materials Research Society, New York, 1985) p. 365.
5. C. T. LIU and V. K. SIKKA, *J. Metals* **38** (1986) 19.
6. V. K. SIKKA, C. T. LIU and E. A. LORIA, in "Enhanced Properties of Structural Metals via Rapid Solidification", edited by F. H. Froes and S. J. Savage (American Society for Metals, Metals Park, OH, 1987) p. 417.
7. J. A. HORTON, C. T. LIU and M. L. SANTELLA, *Metall. Trans.* **18A** (1987).
8. C. T. LIU and C. L. WHITE, *Acta Metall.* **3** (1987) 643.
9. R. N. WRIGHT and V. K. SIKKA, *J. Mater. Sci.* **23** (1988) 4315.

10. M. TAKEYAMA and C. T. LIU, *Acta Metall.* **37** (1989) 2681.
11. M. TAKEYAMA and C. T. LIU, *Scripta Metall.* **23** (1989) 727.
12. W. MATUSZYK, G. CAMUS, D. J. DUQUETTE and N. S. STOLOFF, *Metall. Trans.*, in press.
13. A. K. KURUVILLA and N. S. STOLOFF, *Scripta Metall.* **32** (1987) 873.
14. N. S. STOLOFF, in "High Temperature Ordered Intermetallic Alloys", MRS Symposia 39, edited by C. C. Koch, C. T. Liu and N. S. Stoloff (Materials Research Society, Pittsburgh, PA, 1985) p. 3.
15. G. E. FUCHS and N. S. STOLOFF, *Scripta Metall.* **21** (1987) 863.
16. N. R. BONDA, D. P. POPE and C. LAIRD, *Acta Metall.* **35** (1987) 2371.
17. D. EYLON, Y. MAHAJAN, N. R. ONTKO and F. H. FROES, in "Powder Metallurgy of Titanium Alloys" Proceedings of TMS-AIME Symposium, Las Vegas, NV, 26-28 February, 1980; TMS-AIME, Warrendale, Pa.
18. M. R. MITCHELL, in "Fatigue and Microstructure" (American Society of Metals, Metals Park, Ohio, 1979) p. 406.
19. R. W. LANDGRAF, in "Achievement of High Fatigue Resistance in Metals and Alloys", ASTM Special Technical Publication 467 (American Society for Testing and Materials, Philadelphia, PA, 1969) p. 3.
20. J. D. MORROW, "Cyclic Plastic Strain Energy and Fatigue of Metals", ASTM STP 378, International Friction Damping, and Cyclic Plasticity (American Society of Testing and Materials, Philadelphia, PA, 1965) p. 45.
21. T. S. COOK, *J. Engng Mater. Tech.* **104** (1982) 186.
22. R. W. LANDGRAF, "Cyclic Deformation and Fatigue Behavior of Hardened Steels", Report No. 320, Department of Theoretical and Applied Mechanics, University of Illinois, Urban, IL, November 1968.
23. E. J. KOSINSKI, in "1982 National Powder Metallurgy Conference Proceedings", edited by J. G. Bewley and S. W. McGee, (Metal Powder Industries Federation, Princetown, New Jersey, USA, 1983) p. 491.
24. Y. BIROL, *J. Mater. Sci.* **24** (1989) 2093.
25. S. B. CHAKRABORTY, *Fat. Engng Mater. Str.* **2** (1979) 331.
26. S. MAJUMDAR and J. D. MORROW, in "Fracture Toughness and Slow-Stable Cracking", STP 559 (American Society for Testing and Materials, Philadelphia, PA 1974) p. 159.
27. C. E. FELTNER and C. LAIRD, STP 467 (American Society for Testing and Materials, Philadelphia, PA, 1970) p. 77.
28. C. H. WELLS and C. P. SULLIVAN, *Trans. ASM* **57** (1964) 841.
29. C. CALABRESE and C. LAIRD, *Mater. Sci. Engng* **13** (1974) 141.
30. C. LAIRD, in "Plastic Deformation of Materials", Vol. 16, edited by R. J. Arsenault (Academic Press, New York, 1975) p. 101.
31. D. E. GORDON and C. K. UNNI, presented at ASM Fall Conference, Indianapolis, Indiana, 2-5 October 1989.
32. R. E. STOLTZ and A. G. PINEAU, *Mater. Sci. Engng* **34** (1978) 275.

Received 1 October 1990
and accepted 25 February 1991